Feasibility of using metakaolinite for the treatment of coal-mining acid mine drainage: insights into the interaction behaviour and partitioning of inorganic contaminants

Matome Mothetha[1,2] (ID), Titus Msagati[3], Vhahangwele Masindi[1,4] and Kefeni Kebede[3]

[1]Department of Environmental Sciences, College of Agriculture and Environmental Sciences, University of South Africa (UNISA), PO Box 392, Florida 1710, South Africa

[2]Research and Committees Unit, Legislature Department, City of Ekurhuleni, Private Bag X1069, Germiston 1400, South Africa

[3]Institute for Nanotechnology and Water Sustainability, College of Science, Engineering and Technology, University of South Africa (UNISA), Private Bag X6, Florida 1710, South Africa

[4]Water Research Centre, Smart Places Cluster, Council for Scientific and Industrial Research (CSIR), PO Box 395, Pretoria 0184, South Africa

In this novel study, the efficacy of metakaolinite for the treatment of acid mine drainage (AMD) was evaluated. The optimized parameters included the feedstock dosage and contact time. Experimental results were further explored using inductively coupled plasma–mass spectrometry (ICP–MS), ICP–OES (inductively coupled plasma–optical emission spectroscopy), Fourier transform infrared spectroscopy (FTIR), high-resolution–focused ion beam/scanning electron microscopy (HR–FIB/SEM), energy-dispersive x-ray spectroscopy (EDS), x-ray fluorescence (XRF) and x-ray diffraction (XRD). Optimum conditions were observed to be 45 min of mixing time, ≥ 10 g·L^{-1} of feedstock dosage, i.e., metakaolinite, and ambient temperature and pH. The metal content (Fe, Mn, Cr, Cu, Ni, Pb, Al, and Zn) embedded in AMD matrices were partially removed whilst the level of sulphate was significantly reduced. Chemical species removal efficacies were observed to occur in the following sequence; Cr $\geq$ Zn $\geq$ Cu $\geq$ Pb $\geq$ Mn $\geq$ Ni $\geq$ sulphate $\geq$ Mg $\geq$ Fe, with the following removal percentages: 100, 91.7, 74.6, 65, 38.8, 37.5, 32.3, 13.8, and 8.3%, respectively. Thus metakaolinite proved to be partially effective in the treatment of AMD emanating from coal-mining processes. Furthermore, to enhance the performance of this technology, a polishing technique needs to be coupled or integrated to further remove residual inorganic contaminants, as well as other forms of modification such as the addition of alkaline agents to synthesize the nanocomposite and increase its alkalinizing capabilities.

INTRODUCTION

Acid mine drainage (AMD) or acid rock drainage (ARD) comprises of elevated levels of inorganic contaminants, including Al, Fe, Mn, and sulphate, along with traces of heavy metals (Cu, Ni, Zn, Pb), metalloids (As and Cr), and radionuclides (Amos et al., 2015; Park et al., 2019). AMD emanates from areas where there is mining of coal and gold, amongst other minerals. These chemical species originate from the host rock and associated minerals. They get introduced into water through leaching and other chemical weathering processes (Sheoran et al., 2011a; Sheoran et al., 2011b; Amos et al., 2015). When this effluent is discharged into the environment, it can cause ecological damage if not properly treated. Specifically, AMD can cause receiving environments to be devoid of life; this is mainly attributed to the toxic and hazardous chemical species therein (Kefeni et al., 2017; Naidu et al., 2019; Park et al., 2019; Chen et al., 2021). Furthermore, high electrical conductivity, i.e., due to high levels of total dissolved solids (TDS) and acidic pH impair the ability of the receiving environment to support life, hence highlighting the necessity of treating this wastewater stream. In addition, stringent regulatory frameworks have stipulated requirements for wastewater discharge for different industries (Simate and Ndlovu, 2014; Masindi et al., 2016b; Kefeni et al., 2017).

Various methods have been employed for the treatment of acid mine drainage, and these rely on different technologies such as adsorption, ion exchange, precipitation, filtration, bio-(phyto)-remediation, and crystallization, amongst others (Gazea et al., 1996; Bwapwa et al., 2017; Kefeni et al., 2017; Fernando et al., 2018; Naidu et al., 2019; Park et al., 2019; Ighalo et al., 2022; Masindi et al., 2022b). These technologies have been proven to be effective, but have advantages and disadvantages. Precipitation techniques have a challenge of simultaneously precipitating metals occurring at different concentrations, as well as the production of toxic and highly mineralised sludge that requires proper management and disposal. Furthermore, disposing of the sludge will incur additional costs, making the technology undesirable unless water recovery is the main objective in mine-water treatment. Filtration is energy intensive, and generates brine that requires proper management and disposal. These constraints further hinder the application of AMD treatment technologies, especially for authorities or countries that require zero-liquid-discharge (ZLD) technologies. Crystallization has the challenge of being concentration dependent, and also requires exorbitant amounts of energy. Lastly, ion exchange has been perceived as a promising technology but regenerants from the ion exchange resin pose further ecological threats –hence, this technology is still developing (Masindi et al., 2018a; Masindi et al., 2018b; Agboola, 2019; Naidu et al., 2019; Akinwekomi et al., 2020; Ighalo et al., 2022; Masindi et al., 2022a; Masindi et al., 2022b; Thomas et al., 2022).

Adsorption has emerged as the most promising technology that has been widely employed for the removal of contaminants from different wastewater matrices (Agboola, 2019; Naidu et al., 2019; Akinwekomi et al., 2020). This technology has been validated at different scales and is highly effective. Furthermore, the use of locally available materials, their abundance and cheap cost has further encouraged the application of this material for water depollution (Masindi et al., 2015, 2017). Widely used adsorbents include clay, metal oxides, and their composites (Unuabonah and Taubert, 2014; Vinati et al., 2015; Vardhan et al., 2019; Yadav et al., 2019). Due to their high versatility, agile cation exchange capacity, and high efficacy, clay minerals have been employed for the treatment of multicomponent wastewater streams instead of individual elements such as chromium, arsenic, and sulphate, amongst others (Bradl, 2004; Bhattacharyya and Gupta, 2008; Borisover and Davis, 2015; Han et al., 2019). Contaminants in real wastewater solutions exist with other chemicals, which makes it difficult to remove individual contaminants from a highly mineralised wastewater stream. Hence there is advocacy for a holistic approach that covers a wide range of contaminants. Specifically, bentonite clay has been employed for the treatment of real acid mine drainage, but this is an aluminosilicate material with 2:1 layering and a high cation exchange capacity; other clays such as kaolinite and vermiculite have been employed for the treatment of specific contaminants in industrial effluents (Bhattacharyya and Gupta, 2008; Masindi et al., 2015; Burakov et al., 2018). Kaolinite and its derivative, i.e., metakaolinite, has been employed for the removal of metals from different wastewater matrices, but these adsorbents never been tested on a wider range of contaminants in one wastewater matrix, such as acid mine drainage. The aim of this study was to assess the effectiveness of kaolinite and its derivative, metakaolinite, as adsorbents for removing a wider range of contaminants from acid mine drainage. Furthermore, insights into the interaction behaviour and partitioning of inorganic contaminants was also explored.

MATERIALS AND METHODS

Sample collection

Real AMD was collected from a coal mine in Mpumalanga Province, South Africa. The effluent was seeping through the toe of a coal stockpile. This AMD is concentrated and fully oxidised due to evaporation and exposure to atmospheric oxygen, hence Fe(III) was present in elevated concentrations. Wide-mouth high-density polyethylene (HDPE) bottles were used for sample collection, while the suspended solids and debris were removed by filtration using Macherey-Nagel filter papers (MN 615. Ø125mm). After collection, samples were stored in a portable ice chest and transferred to the laboratory. Metakaolinite ($Al_2Si_2O_7$) was acquired from the material laboratory at the Council for Scientific and Industrial Research (CSIR).

Treatment of AMD: optimisation studies

A batch experimental approach was used for the treatment of AMD using the metakaolinite nanoparticles. The experiments were performed in graded volumetric flasks loaded with 1 000 mL of AMD. The mixtures were mixed at specified intervals and dosages as given below. Overhead stirrers mounted on a Philip and Bird stirrer equipped with 6 propellers were used. Examined ranges of contact time and metakaolinite dosages are given in Table 1.

Experiments were performed in triplicate and results presented as mean values as the standard errors were noted as zero (0). Metakaolinite mass was measured using an analytical balance with a precision of 2 decimal places. The parameters considered in the optimisation studies were: (i) contact time (i.e. duration of

Table 1. The examined ranges for contact time and metakaolinite dosage in treatment of coal AMD treatment (AMD volume 1 000 mL and mixing speed 250 r·min⁻¹)

Experimental run	Contact time (min)	Metakaolinite dosage (g)
1	0	10
2	5	10
3	10	10
4	15	10
5	30	10
6	45	10
7	60	0
8	60	0.5
9	60	1
10	60	2.5
11	60	5
12	60	10
13	60	15

mixing of the metakaolinite with AMD), and (ii) metakaolinite dosage (i.e. metakaolinite mass per AMD volume). The effect of these two main parameters on AMD treatment efficiency was examined by first varying the contact time and then the metakaolinite dosage. Optimum contact time was used to identify the optimum metakaolinite dosage. It should be noted that the. Once the optimum parameters were determined, metakaolinite was used to treat AMD under these optimised conditions.

Contaminant removal efficiency (% removal)

Percentage removal of the contaminants contained in AMD after the metakaolinite treatment was estimated using Eq. 1:

$$\text{Precentage (\%) removal} = (\frac{C_0 - C_e}{C_0}) \text{ x } 100 \qquad (1)$$

where C_0 is the initial concentration of any defined contaminant and C_e is the final concentration of the same contaminant after treatment.

Sample characterisation

To identify the chemical species contained in the examined aqueous samples (AMD, before and after treatment with metakaolinite), as well as to identify the purity of the procured individual materials and the composition of the synthesized nanocomposite and sludge generated from the interaction of the metakaolinite with AMD, different analytical techniques were employed. Analytical equipment was used in an ISO/IEC 17025:2017 accredited laboratory, as discussed below.

Aqueous sample characterisation

For characterisation of the in-situ properties of the AMD, i.e., pH, electrical conductivity (EC) and total dissolved solids (TDS), before and after treatment, a multi-parameter probe (HANNA instrument, HI9828) was used. The chemical species contained in the raw and treated AMD were measured by means of inductively coupled plasma–optical emission spectrometry (ICP–OES) (Agilent Technologies 5110, coupled with Agilent SPS 4 Auto sampler) and inductively coupled plasma mass spectrometry (ICP–MS) (Thermo Scientific's XSERIES 2, coupled with ASX-520 auto sampler). Thermo Fisher Scientific's gallery plus discrete analyser photo spectrometer was used for base metal analyses, as well as sulphates. The listed pieces of equipment were utilised

inter-changeably depending on availability and characterisation needs. National Institute of Standards and Technology (NIST) standard reference materials and quality control procedures were observed during the experiments and analyses. Furthermore, inter-laboratory analysis was done to confirm the results.

Solid sample characterisation

To determine the mineralogical characteristics of the: (i) metakaolinite, and (ii) resultant sludge (from the interaction of the metakaolinite with AMD), x-ray diffraction (XRD) (Panalytical's X'Pert PRO x-ray diffractometer along with Philips PW 1710 diffractometer with graphite secondary monochromatic source) was used. Elemental compositions were ascertained using x-ray fluorescence (XRF) (Thermo Scientific's ARL PERFORM'X Sequential X sequential XRF spectrometer, coupled with the UniQuant software for standardless quantitative analysis). Furthermore, the metals and anion functional groups were determined using Fourier transform infrared spectroscopy (FTIR) (Perkin-Elmer Spectrum 100 FTIR spectrometer coupled with Perkin-Elmer's universal attenuated total reflectance (ATR) sampling accessory with a diamond crystal). To corroborate and complement the XRD and XRF results, the morphological, mapping, and elemental properties were measured using a high-resolution (HR) field emission scanning electron microscope (FE–SEM) (SmartSEM-Auriga) coupled with focused ion beam (FIB) and energy dispersive x-ray spectroscopy (EDS). EDS/SEM and FIB/SEM allow for precise and highly accurate measurements, while high-resolution and undistorted imagery can also be obtained.

RESULTS AND DISCUSSION

Optimisation studies

The effects of the range of contact times and metakaolinite dosages given in Table 1 are discussed below.

Effect of metakaolinite dosage

The effect of metakaolinite dosage on EC, pH, Ca and Mg levels as a function of contact time are shown in Fig. 1.

The metakaolinite dosage (in grams) was observed to have an effect on the concentrations of Ca, Mg and EC, and also pH. As expected, there was a general increase in both pH and Ca levels with an increase in reaction time. Conversely, a minimal decrease in EC and Mg concentration was observed with an increase in dosage. This suggests the removal of dissolved substances, leading to a decrease in dissolved solids and thus EC, while certain interactions likely involving ion exchange may have contributed to the increase in Ca levels. Reduction in Mg and EC may be attributed to the adsorption of Mg ions in exchange for other contaminants in the metakaolinite matrices, specifically through isomorphous substitution. An increase in Ca denotes its leaching from the clay matrices. It was thus decided that a metakaolinite dosage of 10 g should be used in the subsequent optimisation studies. Percentage removal of the main chemical species from AMD as a function of metakaolinite dosage are shown in Fig. 2.

As shown in Fig. 2, there was an increase in removal efficacy (% removal) of inorganic contaminants with an increase in
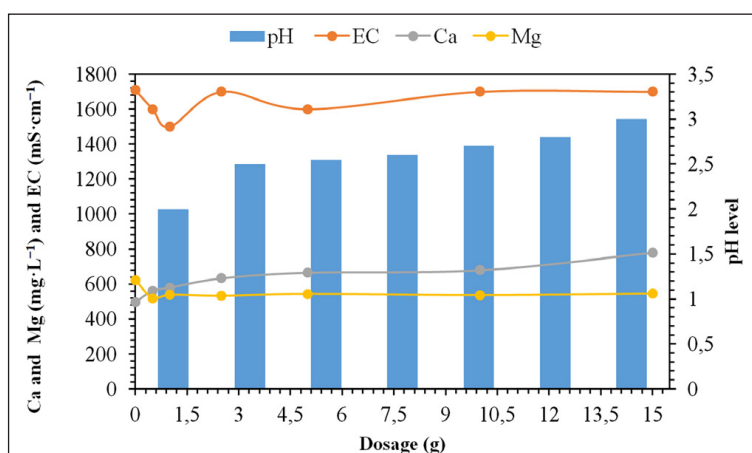

Figure 1. Effects of metakaolinite dosage on EC, pH, Ca, and Mg as a function of contact time (contact time 45 min, AMD volume 1 000 mL, 250 r·min⁻¹ mixing speed, room temperature)
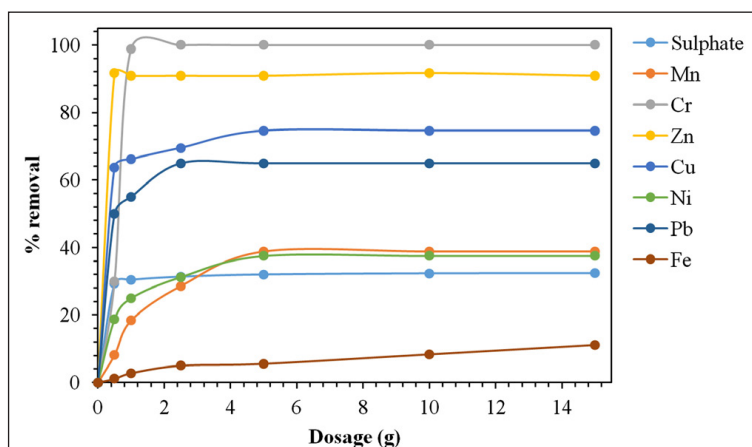

Figure 2. Effects of metakaolinite dosage on the percentage removal of inorganic contaminants (contact time 45 min, AMD volume 1 000 mL, 250 r·min⁻¹ mixing speed, and room temperature)

metakaolinite dosage. An increase in dosage proportionally led to an increase in the number of adsorption sites available for adsorption of contaminants from acid mine drainage. Moreover, the removal of sulphate gradually increased with increasing metakaolinite dosage from 1 g to 15 g, with a maximum removal efficacy of 32%. This could be attributed to the formation of gypsum or any other metal-(oxy)-hydrosulphate when reacting with AMD rich in sulphate (Masindi et al., 2017). Chemical species removal efficiencies were observed to occur in the following sequence; Cr ≥ Zn ≥ Cu ≥ Pb ≥ Ni ≥ Mn ≥ sulphate ≥ Fe, with the following removal percentages 99.9, 91.6, 74.5, 65, 38.7, 37.5, 32.3, and 8%, respectively. Poor removal efficacy for chemical species could be attributed to the lack of enough adsorption and exchange sites on the metakaolinite matrices. This suggests that the main mechanisms that govern the removal of contaminants from AMD using metakaolinite are adsorption and ion exchange. Considering the obtained results, a metakaolinite dosage of 10 g is adequate for the removal of inorganic contaminants from aqueous solutions.

Effect of mixing time

Variation in the levels of EC, pH, Ca, and Mg as a function of contact time are shown in Fig. 3.

As shown in Fig. 3, there was a fluctuating trend in EC and Ca levels with increasing contact time. Initially, Ca levels increased, followed by a subsequent decrease, which may indicate a dynamic interaction between AMD and metakaolinite. The observed fluctuations suggest a possible stoichiometric relationship between the two during the interaction. From 0 to 60 min, the fluctuations in Ca and EC were not directly proportional, indicating complex interactions. Additionally, a reduction in Mg concentration was observed, particularly within the first 5 min, and appeared to correlate with the contact time. The decline in EC further suggests that the reduction in EC is primarily due to attenuation mechanisms, possibly resulting from the leaching of chemical species from the clay interlayers and matrices. Overall, these findings indicate that the reaction between AMD and metakaolinite occurs rapidly and is dependent on contact time. As expected, the pH was also observed to increase with an increase in contact time. The pH increased slightly, i.e., from 2 to 2.57, after 60 min. However, 45 min was taken as the optimum contact time in which to effectively remove the chemical species from AMD. A decrease in Mg implies the exchange of chemical species in the interlayers of clay. Likely mechanisms that could explain the reaction chemistry observed are ion exchange and adsorption.

The variations in the percentage removal of the main chemical species from AMD as a function of mixing time are shown in Fig. 4. As expected, there was an increase in the removal of inorganic contaminants with an increase in contact time (Fig. 4). The removal efficacies were observed to be rapid from 0 to 45 min; thereafter, no significant change was observed during the interaction of AMD and metakaolinite (% removal plateau).
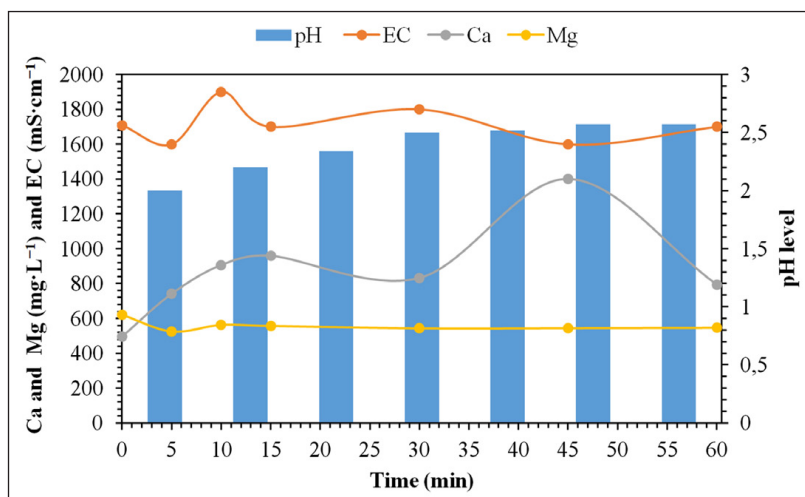

Figure 3. Effects of mixing time on EC, pH, Ca, and Mg (dosage 10 g per 1 000 mL, 250 r·min⁻¹ mixing speed, and room temperature)
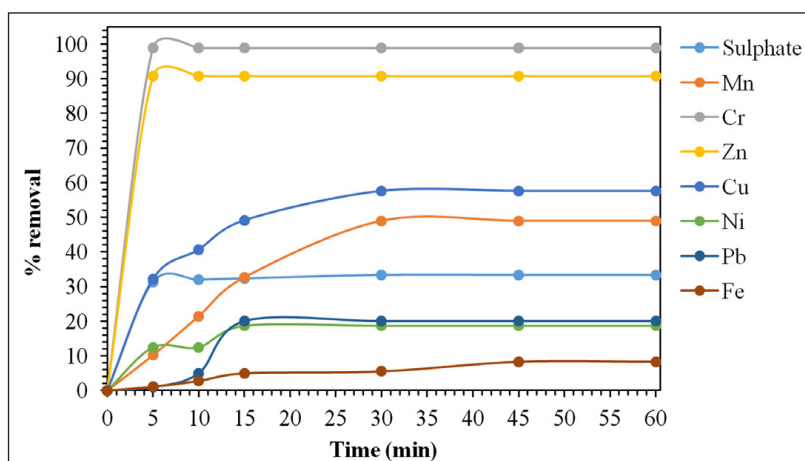

Figure 4. Variations on the percentage removal of inorganic contaminants as a function of contact time (dosage 10 g per 1 000 mL, 250 r·min⁻¹ mixing speed, and room temperature)

As such, 45 min was deemed sufficient for the treatment of AMD with metakaolinite. The chemical species removal efficiencies were observed to occur in the following sequence; Cr ≥ Zn ≥ Cu ≥ Mn ≥ sulphate ≥ Pb ≥ Ni ≥ Fe, with the following removal percentages 98.9, 90.8, 57.6, 48.9, 33.3, 20, 18.8, and 8.3%, respectively. Significant removal of Cr and Zn was observed (≥ 90%). Residual metals and sulphate could be removed using polishing technologies such as adsorption, filtration, ion exchange and bio-(phyto)-remediation. The main objective will be to reclaim water that complies with the prescribed limits. Based on the optimization study, 45 min stands out as the optimum time for both metal and SO$_4$ removal. Lastly, as reported from our previous study (Masindi et al., 2016b, 2017) chemical species were attenuated through different mechanisms such as adsorption, precipitation, complexation, co-precipitation, and co-adsorption, specifically through the formation of gypsum, di-(tri)-metals sulphates, epsomite and oxyhydrosulphates. Results obtained in this study corroborated what has been reported in literature (Meroufel and Zenasni, 2018; Masindi and Ramakokovhu, 2021).

Leaching of Al from metakaolinite matrices

Variation in the leaching of Al ions as a function of contact time and metakaolinite dosage is shown in Fig. 5.

Contrary to other contaminants, the trend for Al ions in the product water was observed to be inversely proportional to the trend for other contaminants. There was a release of Al ions with an increase in dosage and contact time. This could be attributed to the acidic nature of acid mine drainage that enhances the solubility of heavy metals; hence there was leaching of Al from the metakaolinite matrices. A significant amount of Al was observed to be introduced into aqueous solution and this was observed to be proportional to time and dosage. Similar results for kaolinite and its derivative, i.e., metakaolinite, were reported in literature (Kyriakogona et al., 2017; Lin et al., 2018; Karbalaei Saleh et al., 2019; Peng et al., 2021).

Treatment of AMD under optimum conditions

The physicochemical properties of the raw and metakaolinite-treated AMD are reported in Table 2.

After the optimum conditions for contact time and metakaolinite dosage were identified, the AMD was treated under these conditions. As shown in Table 2, although metakaolinite doesn't completely eliminate S and Fe, its application could still offer a practical solution for managing AMD. Metakaolinite treatment significantly reduced the levels of the contaminants contained in AMD, suggesting that it is possible to attenuate and treat real and concentrated AMD. Metakaolinite uses synergies between adsorption, ion exchange, and precipitation, primarily due to the chemical components embedded in its matrices and interlayers.

Table 2. Physicochemical properties of raw and metakaolinite-treated AMD (optimum conditions: 45 min of contact time at 250 r·min⁻¹, 10 g·L⁻¹ of metakaolinite dosage, and room temperature)

Element	Units	AMD	Treated AMD	% removal
Sulphate	mg·L⁻¹	15 000	10 150.0	32.3
Fe	mg·L⁻¹	1 800	1 650.0	8.3
Al	mg·L⁻¹	500	750.0	−50.0
Mn	mg·L⁻¹	98	60.0	38.8
Cr	mg·L⁻¹	0.09	0.0	100.0
Zn	mg·L⁻¹	120	10.0	91.7
Cu	mg·L⁻¹	0.59	0.2	74.6
Ni	mg·L⁻¹	1.6	1.0	37.5
Pb	mg·L⁻¹	0.2	0.1	65.0
Ph	–	2	2.8	−40.0
EC	mS·cm⁻¹	1 709	1 700.0	0.5
Ca	mg·L⁻¹	495	757.0	−52.9
Mg	mg·L⁻¹	622	536.0	13.8

Furthermore, the pH of AMD was observed to increase slightly from 2 to 2.8, indicating that there is no alkalinity released from the metakaolinite matrices to the receiving solution. The chemical species removal efficiencies were observed to occur in the following sequence; Cr ≥ Zn ≥ Cu ≥ Pb ≥ Mn ≥ Ni ≥ sulphate ≥ Mg ≥ Fe, with the following removal percentages: 100, 91.7, 74.6, 65, 38.8, 37.5, 32.3, 13.8, 8.3%, respectively. Chemical species which were observed to leach were Al and Ca. The presence of Fe and S in elevated concentrations implies that the type of mine-water treated in this study emanates from the oxidation of pyrite (Evangelou, 1998).

Solid material characterisation

This section will provide insight on the fate and partitioning of chemical species contained in raw metakaolinite and AMD-reacted metakaolinite (sludge). Results regarding the quality of the treated AMD are corroborated and verified.

Elemental composition

The elemental composition of metakaolinite, and AMD-reacted metakaolinite (resultant sludge) were examined by means of XFR, complemented by HR SEM–EDS. The XRF results are shown in Table 3.

As shown in Table 3, metakaolinite and metakaolinite-AMD resultant sludge comprised Al and Si, hence the name aluminosilicate. After contact with the AMD solution, the
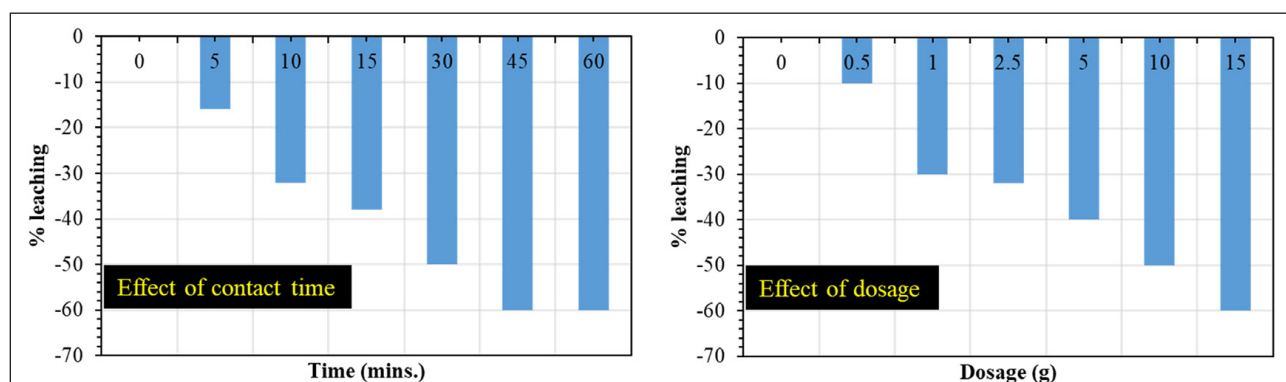

Figure 5. Variation in the leaching of Al ions as a function of contact time and metakaolinite dosage

Table 3. Elemental composition of metakaolinite and AMD-reacted metakaolinite (resultant sludge) as ascertained by the XRF technique

Wt. %.	Standard		Characterisation	
	BHVO-1 STD	BHVO-1 analysed	Metakaolinite	AMD-reacted metakaolinite
SiO_2	49.94	48.17	49.69	43.19
Al_2O_3	13.8	17.33	39.26	37.00
MgO	7.23	5.96	0.72	1.59
Na_2O	2.26	2.94	<0.01	<0.01
P_2O_5	0.273	0.31	0.10	0.08
Fe_2O_3	12.23	10.98	1.32	2.94
K_2O	0.52	0.57	0.41	0.39
CaO	11.4	10.82	1.89	2.11
TiO_2	2.71	2.50	1.52	1.47
V_2O_5	0.0566	0.06	0.01	0.02
Cr_2O_3	0.0422	0.04	0.07	0.06
MnO	0.168	0.17	0.01	0.03
NiO	0.0154	0.01	0.02	0.01
CuO	0.017	0.02	0.01	<0.01
ZrO_2	0.0242	0.02	0.28	0.24
SO_3	–	0.01	0.02	4.01
Nb_2O_5	–	–	0.04	0.04
Co_3O_4	–	0.02	<0.01	0.01
ZnO	–	–	0.01	0.01
SrO	–	0.04	0.03	0.02
Y_2O_3	–	–	0.03	0.03
LOI	–	–	4.50	6.71

resultant sludge comprised elements which are prevalent in AMD and metakaolinite. Specifically, the resultant sludge had elevated levels of Fe, Mg, and S. The detected elements are the major contaminants in AMD, affirming that metakaolinite is acting as a sink of major and trace contaminants from AMD. Their reduction in Al and Si in the resultant metakaolinite-AMD sludge suggests the feasibility of leaching. This finding corroborates the ICP–MS results as reported in the optimization studies. There was a shift in the level of trace elements, but this was insignificant. The loss on ignition (LOI) was also observed to be high. This could be from the loss of water, since this material is hydrated, and to a lesser extent volatile compounds, organic matter, and carbonates.

Map sum spectrums

To complement the XRF results, the HR–FIB/SEM–EDS spectrums for metakaolinite and metakaolinite-AMD sludge were also determined. The corresponding spectrums along with the estimated elemental compositions are shown in Fig. 6.

As shown in Fig. 6, metakaolinite comprised Al and Si as major elements, hence the name aluminosilicate. After contact with the AMD solution, the resultant sludge comprised elements which are prevalent in AMD and metakaolinite. Specifically, the resultant sludge comprised elevated levels of Fe, Mg, and S, confirming that metakaolinite is acting as a sink of major and trace contaminants from real AMD. The obtained results confirmed those from XRF. However, elevated levels of Al and Si were initially observed, but these levels were subsequently reduced, confirming the feasibility of leaching, as indicated by the ICP–MS/OES results. There was a shift in the level of trace elements but this was observed to be very slight.

Morphological and microstructural properties

The morphological and microstructural properties of (a) metakaolinite and (b) metakaolinite-AMD resultant sludge are shown in Fig. 7a–b. To attain high-resolution imagery with limited distortion, HR–FE–SEM was used.

The metakaolinite was observed to comprise heterogeneous mixtures of leaf-like petals and layers, and show hexagonal platelets connected to each other (Fig. 7a). The microstructural properties were observed to be the same at different magnifications. Similar results were reported in literature (Konan et al., 2009). The metakaolinite-AMD resultant sludge was also observed to comprise leaf-like and hexagonal structures but was dominated by rod-like structures. The results confirm the microstructural transformation of the material and this confirms that there is deposition of new mineral phases in the sludge from AMD (Fig. 7b). This further corroborates the removal and dissolution of contaminants from the interaction between AMD and metakaolinite.

Elemental distribution mapping using EDS

To further corroborate the XRF and the SEM/EDS results regarding the elemental composition of the solid samples, elemental distribution mapping was also carried out using the FE–SEM instrument's EDS capabilities. Results are shown in Fig. 8.

As shown in Fig. 8a, the metakaolinite comprised Al, O and Si as dominant elements along with trace levels of Mg, Ca and K. The elements were evenly distributed across the surface. The distribution of these elements on the surface of the material further confirms the nature of the material, i.e., aluminosilicate. The obtained results correspond to that found using XRF and EDS. The resultant sludge produced from the interaction of metakaolinite with AMD (Fig. 8b) comprised Al, Si, Fe, S, K, and Ca as predominant elements. The obtained results corroborate those from the ICP–MS/OES analyses of the raw and product water quality, and this demonstrates the fate of chemical components after treatment of AMD with metakaolinite.
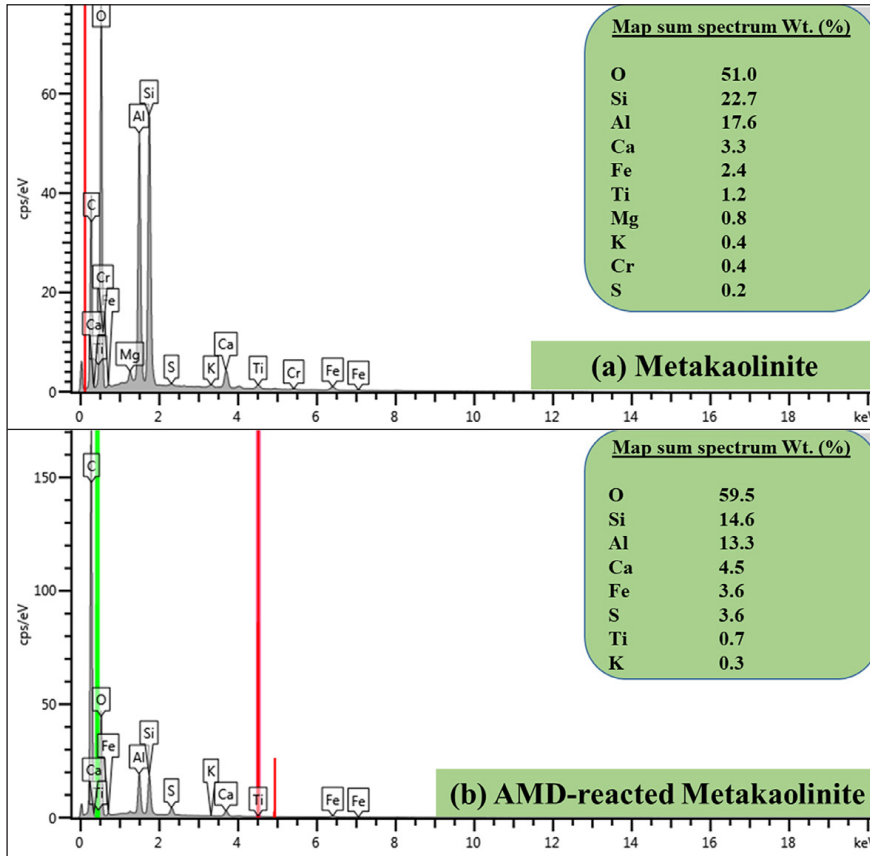
Figure 6. Elemental composition of (a) metakaolinite and (b) metakaolinite-AMD sludge using EDS/SEM spectrums
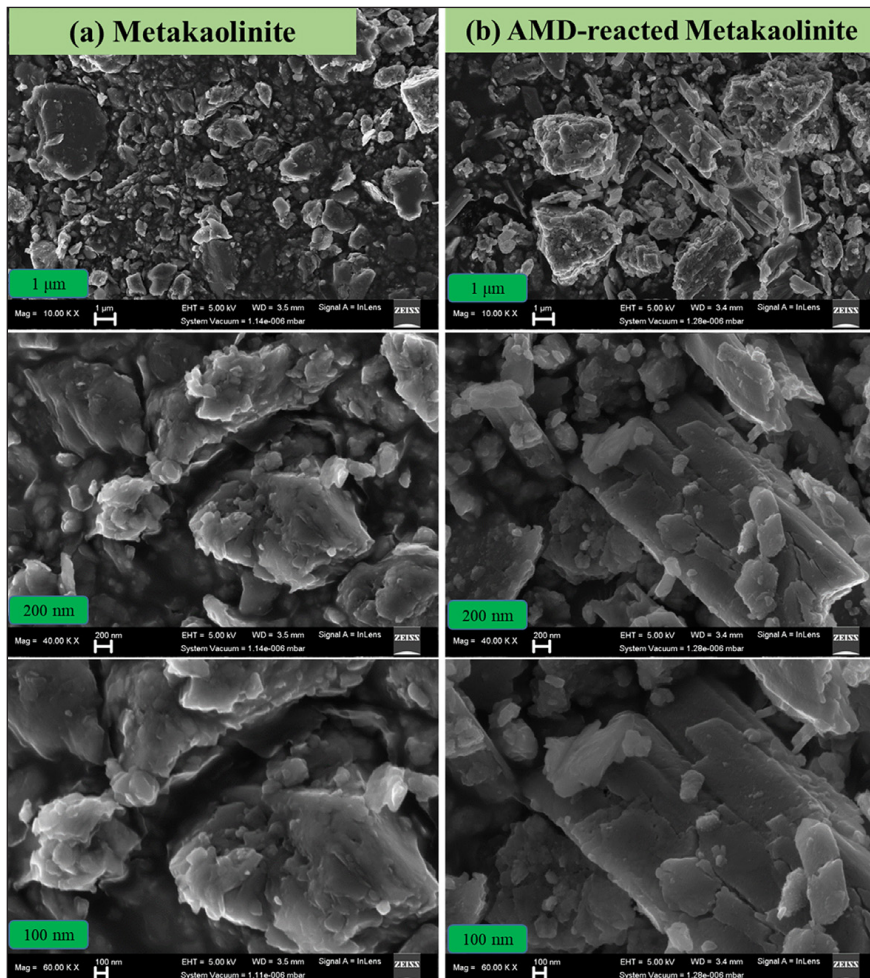

Figure 7. The morphological and microstructural properties of (a) metakaolinite and (b) metakaolinite-AMD resultant sludge
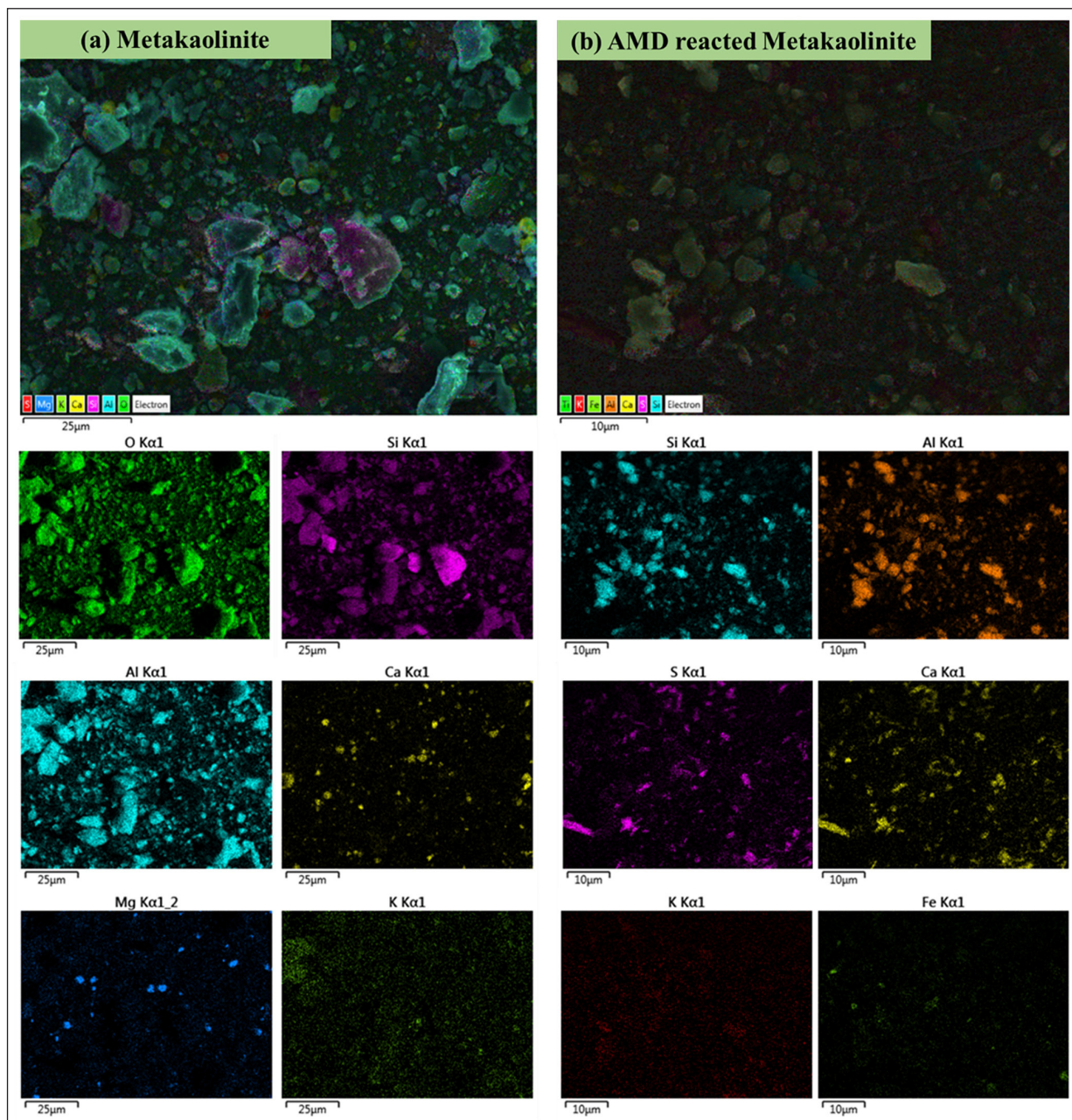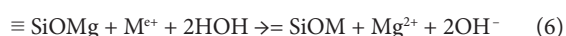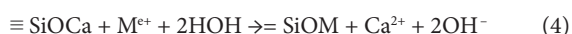
Figure 8. EDS/SEM imagery and elemental maps of (a) metakaolinite and (b) metakaolinite-AMD resultant sludge

Mineralogical properties

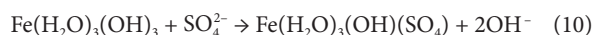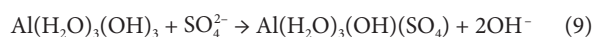The mineralogical composition and crystal phases of the examined solid samples were identified using XRD (Fig. 9).

Metakaolinite comprised mullite, quartz, cristobalite, hematite, kaolinite, rutile, and calcite on its matrices. This confirms that this mineral is an aluminosilicate material with other impurities. However, chemicals embodied in its matrices could justify certain chemical reactions, specifically, the silicate will react with acidity in AMD via ion exchange, hence increasing the pH of the product water (Eqs 2–6) (Masindi et al., 2015).

$$\equiv SiOH \leftrightarrow SiO^- + H^+ \tag{2}$$

$$\equiv SiOH + Ca^{2+} \leftrightarrow= SiOCa + H^+ \tag{3}$$

$$\equiv SiOCa + M^{e+} + 2HOH \rightleftharpoons= SiOM + Ca^{2+} + 2OH^- \tag{4}$$

$$\equiv SiOH + Mg^{2+} \leftrightarrow= SiOMg + H^+ \tag{5}$$

$$\equiv SiOMg + M^{e+} + 2HOH \rightleftharpoons= SiOM + Mg^{2+} + 2OH^- \tag{6}$$

The metakaolinite-AMD resultant sludge comprised mullite, quartz, cristobalite, hematite, kaolinite, rutile, and basanite. The noisy signal in the spectrogram of the resultant sludge denotes the presence of amorphous phases in its matrix . The reaction of basanite in the metakaolinite matrices (interlayers) and AMD is in agreement with the XRD, EDS mapping, and XRF, and this could be explained by the following equations (Masindi et al., 2016a):

$$CaO + H_2O \rightarrow Ca(OH)_2 \tag{7}$$

$$MgSO_4 + Ca\,(OH)_2 \rightarrow Mg\,(OH)_2 + CaSO_4 \tag{8}$$
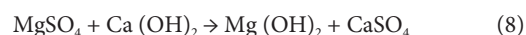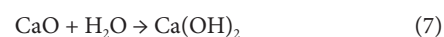
The presence of new phases, i.e., basanite, demonstrates the decomposition of metakaolinite and the formation of new mineral phases. The disappearance of calcite confirms the alkalinity in the product water as explained in Eqs 9–10.

$$Al(H_2O)_3(OH)_3 + SO_4^{2-} \rightarrow Al(H_2O)_3(OH)(SO_4) + 2OH^- \tag{9}$$

$$Fe(H_2O)_3(OH)_3 + SO_4^{2-} \rightarrow Fe(H_2O)_3(OH)(SO_4) + 2OH^- \tag{10}$$

The result from this study corroborates what has been reported in ICP–MS/OES, and SEM–EDS.
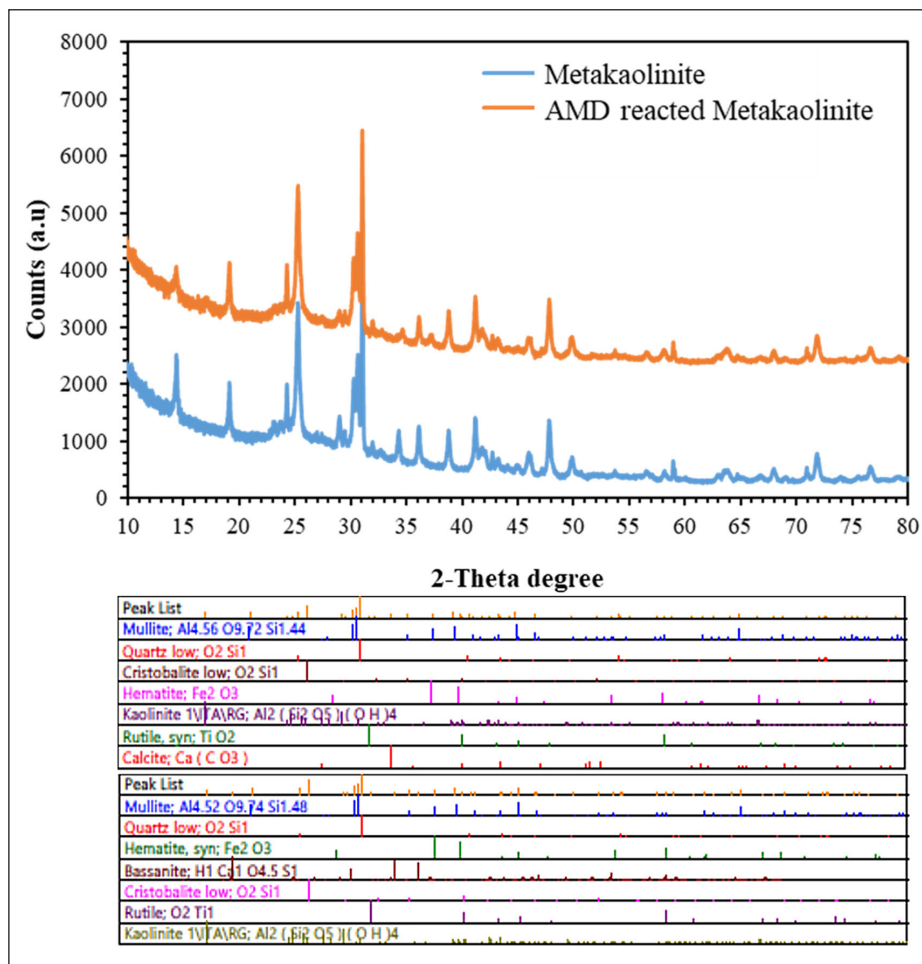
Figure 9. Mineralogical composition of the metakaolinite, and metakaolinite-AMD resultant sludge
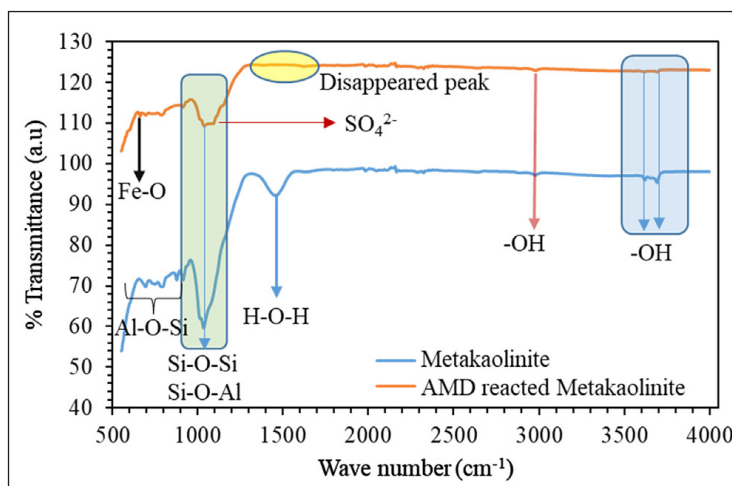

Figure 10. The FTIR spectrum of the metakaolinite and metakaolinite-AMD resultant sludge

Functional groups

The FTIR spectrums of the solid samples were also identified, along with their functional groups and wavenumbers (cm⁻¹). The results for metakaolinite and metakaolinite-AMD resultant sludge are shown in Fig. 10.

As shown in Fig. 10, the obtained FTIR results corroborate the XRF, XRD, and EDS/SEM results. It appears that the use of metakaolinite, can provide an innovative option for the treatment of AMD. With this treatment method, effective management of AMD from coal mining can be achieved, while water could also be reclaimed

using polishing techniques. This is of particular importance for South Africa and other countries and areas that are affected by water scarcity and AMD-producing mining activities. Raw metakaolinite comprised Al–O–Si, Si–O–Si, and H–O–H peaks. The obtained results are consistent with what has been reported in literature (Srivastava et al., 2005; Tang and Shih, 2012; Wainipee et al., 2013; Zhao and He, 2014). This shows that the material is an aluminosilicate that is hydrated. However, after the interaction of metakaolinite with AMD, peaks for elements in AMD were observed in the resultant sludge, including S and Fe, confirming that metakaolinite is a sink for chemicals found in AMD.

CONCLUSIONS

This study successfully proved the effectiveness of metakaolinite in treating AMD arising from coal-mining processes. The obtained results were confirmed with a variety of analytical techniques and instruments, such as FTIR, HR-FIB/SEM, EDS, XRF, and XRD. Optimum conditions were observed to be 45 min of mixing time, ≥ 10 g·L^{-1} of metakaolinite dosage and ambient temperature and pH. The metal content (Fe, Mn, Cr, Cu, Ni, Pb, Al, and Zn) embedded in AMD matrices was partially reduced. Chemical species removal efficiencies were observed to occur in the following sequence; Cr ≥ Zn ≥ Cu ≥ Pb ≥ Mn ≥ Ni ≥ sulphate ≥ Mg ≥ Fe, with the following removal percentages 100, 91.7, 74.6, 65, 38.8, 37.5, 32.3, 13.8, 8.3%, respectively. The fate of the chemicals contained in the AMD were observed in the generated sludge after the interaction with metakaolinite. Moreover, metakaolinite was observed to leach Al and Si into the product water. This treatment approach holds great promise for the sustainable management of AMD effluents from coal-mining activities and can provide a simple and effective solution for AMD management. Neutralisation, softening and filtration technologies will need to be coupled to this process to further enhance the reclamation of drinking water and to explore possible recovery of valuable minerals from the generated sludge.

AUTHOR CONTRIBUTIONS

M Mothetha: conceptualization, validation, formal analysis, investigation, resources, data curation, writing – original draft, writing – review and editing, visualization, and project administration. K Kefeni: supervision, conceptualization, validation, formal analysis, investigation, data curation, and writing – review and editing, visualization. V Masindi: supervision, conceptualization, validation, formal analysis, investigation, data curation, and writing – review and editing, visualization. T Msagati: supervision, conceptualization, validation, formal analysis, investigation, data curation, writing – review and editing, and funding acquisition.

ACKNOWLEDGEMENTS

ORCID

Matome Mothetha
https://orcid.org/0000-0003-1506-5926

REFERENCES

AGBOOLA O (2019) The role of membrane technology in acid mine water treatment: a review. *Kor. J. Chem. Eng.* **36** 1389–1400. https://doi.org/10.1007/s11814-019-0302-2

AKINWEKOMI V, MAREE JP, MASINDI V, ZVINOWANDA C, OSMAN MS, FOTEINIS S, MPENYANA-MONYATSI L and CHATZISYMEON E (2020) Beneficiation of acid mine drainage (AMD): A viable option for the synthesis of goethite, hematite, magnetite, and gypsum – gearing towards a circular economy concept. *Miner. Eng.* **148** 106204. https://doi.org/10.1016/j.mineng.2020.106204

AMOS RT, BLOWES DW, BAILEY BL, SEGO DC, SMITH L and RITCHIE AIM (2015) Waste-rock hydrogeology and geochemistry. Appl. Geochem. 57 140–156. https://doi.org/10.1016/j.apgeochem.2014.06.020

BHATTACHARYYA KG and GUPTA SS (2008) Adsorption of a few heavy metals on natural and modified kaolinite and montmorillonite: A review. *Adv. Colloid Interf. Sci.* **140** 114–131. https://doi.org/10.1016/j.cis.2007.12.008

BORISOVER M and DAVIS JA (2015) Chapter 2. Adsorption of inorganic and organic solutes by clay minerals. In: Tournassat C, Steefel CI, Bourg IC and Bergaya F (eds.) *Developments in Clay Science.* 33–70. https://doi.org/10.1016/B978-0-08-100027-4.00002-4

BRADL HB (2004) Adsorption of heavy metal ions on soils and soils constituents. *J. Colloid Interf. Sci..* **277** 1–18. https://doi.org/10.1016/j.jcis.2004.04.005

BURAKOV AE, GALUNIN EV, BURAKOVA IV, KUCHEROVA AE, AGARWAL S, TKACHEV AG and GUPTA VK (2018) Adsorption of heavy metals on conventional and nanostructured materials for wastewater treatment purposes: A review. *Ecotoxicol. Environ. Saf..* **148** 702–712. https://doi.org/10.1016/j.ecoenv.2017.11.034

BWAPWA JK, JAIYEOLA AT and CHETTY R (2017) Bioremediation of acid mine drainage using algae strains: A review. *S. Afr. J. Chem. Eng.* **24** 62–70. https://doi.org/10.1016/j.sajce.2017.06.005

CHEN G, YE Y, YAO N, HU N, ZHANG J and HUANG Y (2021) A critical review of prevention, treatment, reuse, and resource recovery from acid mine drainage. *J. Cleaner Prod.* **329** 129666. https://doi.org/10.1016/j.jclepro.2021.129666

EVANGELOU VP (1998) Pyrite chemistry: the key for abatement of acid mine drainage. In: Geller W, Klapper H and Salomons W (eds) *Acidic Mining Lakes: Acid Mine Drainage, Limnology and Reclamation.* Springer, Berlin.

FERNANDO WAM, ILANKOON IMSK, SYED TH and YELLISHETTY M (2018) Challenges and opportunities in the removal of sulphate ions in contaminated mine water: A review. *Miner. Eng.* **117** 74–90. https://doi.org/10.1016/j.mineng.2017.12.004

GAZEA B, ADAM K and KONTOPOULOS A (1996) A review of passive systems for the treatment of acid mine drainage. *Miner. Eng.* **9** 23–42. https://doi.org/10.1016/0892-6875(95)00129-8

HAN H, RAFIQ MK, ZHOU T, XU R, MAŠEK O and LI X (2019) A critical review of clay-based composites with enhanced adsorption performance for metal and organic pollutants. *J. Hazardous Mater.* **369** 780–796. https://doi.org/10.1016/j.jhazmat.2019.02.003

IGHALO JO, KURNIAWAN SB, IWUOZOR KO, ANIAGOR CO, AJALA OJ, OBA SN, IWUCHUKWU FU, AHMADI S and IGWEGBE CA (2022) A review of treatment technologies for the mitigation of the toxic environmental effects of acid mine drainage (AMD). *Process Saf. Environ. Protect.* **157** 37–58. https://doi.org/10.1016/j.psep.2021.11.008

KARBALAEI SALEH D, ABDOLLAHI H, NOAPARAST M and FALLAH NOSRATABAD A (2019) Dissolution of aluminium from metakaolin with oxalic, citric and lactic acids. *Clay Miner.* **54** 209–217. https://doi.org/10.1180/clm.2019.28

KEFENI KK, MSAGATI TAM and MAMBA BB (2017) Acid mine drainage: Prevention, treatment options, and resource recovery: A review. *J. Cleaner Prod.* **151** 475–493. https://doi.org/10.1016/j.jclepro.2017.03.082

KONAN KL, PEYRATOUT C, SMITH A, BONNET JP, ROSSIGNOL S and OYETOLA S (2009) Comparison of surface properties between kaolin and metakaolin in concentrated lime solutions. *J. Colloid Interf. Sci.* **339** 103–109. https://doi.org/10.1016/j.jcis.2009.07.019

KYRIAKOGONA K, GIANNOPOULOU I and PANIAS D (2017) Extraction of aluminium from kaolin: a comparative study of hydrometallurgical processes. In: *Proceedings of the 3rd World Congress on Mechanical, Chemical, and Material Engineering* **17** 8–10. https://doi.org/10.11159/mmme17.133

LIN M, LIU YY, LEI SM, YE Z, PEI ZY and LI B (2018) High-efficiency extraction of Al from coal-series kaolinite and its kinetics by calcination and pressure acid leaching. *Appl. Clay Sci.* **161** 215–224. https://doi.org/10.1016/j.clay.2018.04.031

MASINDI V, CHATZISYMEON E, KORTIDIS I and FOTEINIS S (2018a) Assessing the sustainability of acid mine drainage (AMD) treatment in South Africa. *Sci. Total Environ.* **635** 793–802. https://doi.org/10.1016/j.scitotenv.2018.04.108

MASINDI V, FOSSO-KANKEU E, MAMAKOA E, NKAMBULE TTI, MAMBA BB, NAUSHAD M and PANDEY S (2022a) Emerging remediation potentiality of struvite developed from municipal wastewater for the treatment of acid mine drainage. *Environ. Res.* **210** 112944. https://doi.org/10.1016/j.envres.2022.112944

MASINDI V, FOTEINIS S and CHATZISYMEON E (2022b) Co-treatment of acid mine drainage and municipal wastewater effluents: Emphasis on the fate and partitioning of chemical contaminants. *J. Hazardous Mater.* **421** 126677. https://doi.org/10.1016/j.jhazmat.2021.126677

MASINDI V, GITARI MW, TUTU H and DE BEER M (2016a) Fate of inorganic contaminants post treatment of acid mine drainage by cryptocrystalline magnesite: Complimenting experimental results with a geochemical model. *J. Environ. Chem. Eng.* **4** 4846–4856. https://doi.org/10.1016/j.jece.2016.03.020

MASINDI V, GITARI MW, TUTU H and DEBEER M (2015) Efficiency of ball milled South African bentonite clay for remediation of acid mine drainage. *J. Water Process Eng.* **8** 227–240. https://doi.org/10.1016/j.jwpe.2015.11.001

MASINDI V, GITARI MW, TUTU H and DEBEER M (2017) Synthesis of cryptocrystalline magnesite–bentonite clay composite and its application for neutralization and attenuation of inorganic contaminants in acidic and metalliferous mine drainage. *J. Water Process Eng.* **15** 2–17. https://doi.org/10.1016/j.jwpe.2015.11.007

MASINDI V, CHATZISYMEON E, KORTIDIS I and FOTEINIS S (2018a) Assessing the sustainability of acid mine drainage (AMD) treatment in South Africa. *Sci. Total Environ.* **635** 793-802. https://doi.org/10.1016/j.scitotenv.2018.04.108

MASINDI V, MADZIVIRE G and TEKERE M (2018b) Reclamation of water and the synthesis of gypsum and limestone from acid mine drainage treatment process using a combination of pre-treated magnesite nanosheets, lime, and CO_2 bubbling. *Water Resour. Ind.* **20** 1–14. https://doi.org/10.1016/j.wri.2018.07.001

MASINDI V, OSMAN MS, MBHELE RN and RIKHOTSO R (2016b) Fate of pollutants post treatment of acid mine drainage with basic oxygen furnace slag: Validation of experimental results with a geochemical model. *J. Cleaner Prod.* **172** 2899–2909. https://doi.org/10.1016/j.jclepro.2017.11.124

MASINDI V and RAMAKOKOVHU MM (2021) The performance of thermally activated and vibratory ball milled South African bentonite clay for the removal of chromium ions from aqueous solution. *Mater. Today Proc.* **38**. 964–974. https://doi.org/10.1016/j.matpr.2020.05.490

MEROUFEL B and ZENASNI MA (2018) Preparation, characterization, and heavy metal ion adsorption property of APTES-modified kaolin: comparative study with original clay. In: Hussain CM (ed.) *Handbook of Environmental Materials Management*. Springer, Cham.

NAIDU G, RYU S, THIRUVENKATACHARI R, CHOI Y, JEONG S and VIGNESWARAN S (2019) A critical review on remediation, reuse, and resource recovery from acid mine drainage. *Environ. Pollut.* **247** 1110–1124. https://doi.org/10.1016/j.envpol.2019.01.085

PARK I, TABELIN CB, JEON S, LI X, SENO K, ITO M and HIROYOSHI N (2019) A review of recent strategies for acid mine drainage prevention and mine tailings recycling. *Chemosphere* **219** 588–606. https://doi.org/10.1016/j.chemosphere.2018.11.053

PENG H, QI T, VOGRIN J, HUANG Q, WU W and VAUGHAN J (2021) The effect of leaching temperature on kaolinite and meta-kaolin dissolution and zeolite re-precipitation. *Miner. Eng.* **170** 107071. https://doi.org/10.1016/j.mineng.2021.107071

SHEORAN AS, SHEORAN V and CHOUDHARY RP (2011a) Geochemistry of acid mine drainage: A review. *Perspect. Environ. Res.* **4** 293.

SHEORAN V, SHEORAN A and CHOUDHARY RP (2011b) Biogeochemistry of acid mine drainage formation: A review. *Mine Drain. Related Problems* 119–154. https://doi.org/10.3923/jest.2012.119.127

SIMATE GS and NDLOVU S (2014) Acid mine drainage: Challenges and opportunities. *Journal of Environ. Chem. Eng.* **2** 1785–1803. https://doi.org/10.1016/j.jece.2014.07.021

SRIVASTAVA P, SINGH B and ANGOVE M (2005) Competitive adsorption behavior of heavy metals on kaolinite. *J. Colloid Interf. Sci.* **290** 28–38. https://doi.org/10.1016/j.jcis.2005.04.036

TANG Y and SHIH K (2012) Applying kaolinite-mullite reaction series to immobilize toxic metals in environment. In: Orbovic V and Huang Z (eds) *Kaolinite: Occurrences, Characteristics and Applications*. Nova Science Publishers, New York. 69-97. http://hdl.handle.net/10722/160964

THOMAS G, SHERIDAN C and HOLM PE (2022) A critical review of phytoremediation for acid mine drainage-impacted environments. *Sci. Total Environ.* **811** 152230. https://doi.org/10.1016/j.scitotenv.2021.152230

UNUABONAH EI and TAUBERT A (2014) Clay–polymer nanocomposites (CPNs): Adsorbents of the future for water treatment. *Appl. Clay Sci.* **99** 83–92. https://doi.org/10.1016/j.clay.2014.06.016

VARDHAN KH, KUMAR PS and PANDA RC (2019) A review on heavy metal pollution, toxicity and remedial measures: Current trends and future perspectives. *J. Mol. Liq.* **290** 111197. https://doi.org/10.1016/j.molliq.2019.111197

VINATI A, MAHANTY B and BEHERA SK (2015) Clay and clay minerals for fluoride removal from water: A state-of-the-art review. *Appl. Clay Sci.* **114** 340–348. https://doi.org/10.1016/j.clay.2015.06.013

WAINIPEE W, CUADROS J, SEPHTON MA, UNSWORTH C, GILL MG, STREKOPYTOV S and WEISS DJ (2013) The effects of oil on As(V) adsorption on illite, kaolinite, montmorillonite and chlorite. *Geochim. Cosmochim. Acta.* **121** 487–502. https://doi.org/10.1016/j.gca.2013.07.018

YADAV VB, GADI R and KALRA S (2019) Clay based nanocomposites for removal of heavy metals from water: A review. *J. Environ. Manage.* **232** 803–817. https://doi.org/10.1016/j.jenvman.2018.11.120

ZHAO J and HE MC (2014) Theoretical study of heavy metal Cd, Cu, Hg, and Ni(II) adsorption on the kaolinite(0 0 1) surface. *Appl. Surf. Sci.* **317** 718–723. https://doi.org/10.1016/j.apsusc.2014.08.162